Photoprocesses in Self-Assembled Complexes of Oligopeptides with Metalloporphyrins

Mohamed Aoudia and Michael A. J. Rodgers*

Contribution from the Center for Photochemical Sciences, Department of Chemistry, Bowling Green State University, Bowling Green, Ohio 43403

Received July 23, 1997[⊗]

Abstract: Ion-pair complexes between the cationic metalloporphyrins, tetrakis(*N*-methyl-4-pyridyl)porphyrin (Pd(II)TMPyP^{4+} and Zn(II)TMPyP^{4+}), and anionic pentapeptides consisting of a string of four glutamic acid residues terminated either by tyrosine (Glu4Tyr) or by tryptophan moieties (Glu4Trp) have been assembled and studied by steady-state and time-resolved spectroscopy. Evidence for ion association between porphyrin and peptide was provided by the effect of peptide concentration on the ground state absorption spectra of the porphyrin. Flash photolysis experiments showed that, in the presence of peptide, Pd(II)TMPyP^{4+} triplet decay was described by the sum of two exponential terms. The fast decay component ($6.6 \pm 0.2\ 10^6\ s^{-1}$ for the Tyr variant and $1.4 \pm 0.15\ 10^7\ s^{-1}$ for the Trp analog) was found to be independent of peptide concentration. The slow decay component showed a linear increase in value with peptide concentration, and a bimolecular rate constant of $6.2 \times 10^9\ M^{-1}\ s^{-1}$ was extracted for both peptides. The fast contribution to the T_1 decay was associated with an intracomplex electron transfer, whereas the slow contribution was associated with the diffusive formation of an encounter complex between free peptide and porphyrin molecules (bulk phase) followed by electron transfer. Evidence for this intracomplex electron transfer reaction was derived from the study of the effect of pH-induced alteration of the fast rate component. An increase of the rate constant resulted from the pH-governed increases in ΔE^0 for oxidation. However, at pH values >8.5, although the driving force continued to increase, the rate constant reached a limiting value and became pH-independent ($10^7\ s^{-1}$ for the Tyr residue and $2.4 \times 10^7\ s^{-1}$ for Trp). To explain this, a mechanism was invoked in which segmental diffusion within the porphyrin−peptide complex is supposed to precede the electron transfer step, this putative diffusion requirement becoming rate-determining at high pH (high driving force). Additional evidence for electron transfer within the ion-pair complex was obtained when Zn(II)TMPyP^{4+} was used as the redox partner.

Introduction

The transfer of an electron from one site to another within a protein matrix is critical to the function of a wide range of biological processes, and understanding of the detail of such has become one of the outstanding experimental[1] and theoretical[2] challenges of the last decades of the twentieth century. Taking the respiratory system as an example, electrons are caused to move distances of 20 Å or more between a heme cofactor within one protein to another cofactor in an adjoining unit.[3−7] Detailed investigations have revealed that the protein itself does not simply act as an inert supporting bystander;[8] rather, it is widely held that the molecular nature of the protein serves to have a modulating effect on the rate of the process.[9−11] Thus, evidence exists that structural motifs such as β-sheets act to facilitate the process more than do α-helices, for example.[12] It is also becoming apparent that the cofactor−protein interaction is not of a static nature, but that motional dynamics occur after docking and prior to electron transfer which can serve to assist the transfer of charge.[13]

Earlier work from this laboratory provided additional evidence for the role played by local dynamics in small molecule−protein interactions.[14] Self-assembled ion pairs between cytochrome *c* and a series of uroporphyrins were photoexcited to provide the system with the driving force for intracomplex electron transfer between the reaction partners. The complexes were assembled prior to excitation by taking advantage of the cationic lysine patch on the protein surface in the vicinity of the heme cleft,

* To whom correspondence should be addressed. Phone: 419-372-7606. Fax: 419-372-9300. E-mail: rodgers@bgnet.bgsu.edu.

⊗ Abstract published in *Advance ACS Abstracts,* December 15, 1997.

(1) (a) *Electron Transfer in Inorganic, Organic and Biological Systems;* Bolton, J. R., Mataga, N., McLendon, G., Eds.; Advances in Chemistry 228; American Chemical Society: Washington, DC, 1991. (b) *Long-Range Electron Transfer in Biology;* Palmer, G., Ed.; Springer-Verlag: Berlin, 1991; Vol. 75. (c) McLendon, G. *Chem. Res.* **1988**, *21*, 160. (d) *Electron Transfer in Biology and the Solid State;* Johnson, M. K., King, R. B., Kurtz, D. M., Jr., Kutal, C., Norton, M. L., Scott, R. A., Eds.; American Chemical Society: Washington, DC, 1990. (e) Winkler, J. R.; Gray, H. B. *Chem. Rev.* **1992**, 369. (f) Gray, H. B.; Malmström, Bo-G. *Biochemistry* **1989**, *19*, 7499. (g) Moser, C. C.; Dutton, P. L. In *Protein Electron Transfer*; Bendall, D. S., Ed.; Bios Scientific Publishers: Oxford, 1996; pp 1−21.

(2) (a) Marcus, R. J. *J. Chem. Phys.* **1956**, *24*, 966. (b) Marcus, R. J.; Sutin, N. *Biochim. Biophys. Acta* **1985**, *811*, 265. (c) Jortner, J.; Bixon, M. In *Protein Structure: Molecular and Electronic Reactivity;* Austin, R., Buhks, E., Chance, B., DeVault, D., Dutton, P. L., Frauenfelder, H., Gol'danskii, V. I., Eds.; Springer-Verlag: New York, 1987; pp 277−308. (d) Bixon, M.; Jortner, J.; Michel-Beyerle, M. E.; Ogrodnik, A. *Biochim. Biophys. Acta* **1989**, *977*, 273.

(3) *Tunnelling in Biological Systems;* Chance, B., DeVault, D. C., Frauenfelder, H., Marcus, R. A., Schrieffer, J. R., Sutin, N., Eds.; Academic: New York, 1979.

(4) Hatefi, Y. *Annu. Rev. Biochem.* **1985**, *54*, 1505.

(5) Dixit, B. P. S. N.; Vanderkooi, J. M. *Curr. Top. Bioenerg.* **1984**, *13*, 159.

(6) *Antennas in Reaction Centers of Photosynthetic Bacteria;* Michel-Beyerle, M. E., Ed.; Springer-Verlag: Berlin, 1985.

(7) *Photosynthesis: Energy Conversion by Plants and Bacteria;* Govindjee, Ed.; Academic: New York, 1982; Vol. I.

(8) Gray, H. B. *Aldrichim. Acta* **1990**, *23*, 87.

(9) Beretan, D. N.; Betts, J. N.; Onuchic, J. N. *Science* **1991**, *252*, 1285.

(10) Onuchic, J. N.; Beratan, D. N; Gray, H. B. *Annu. Rev. Biophys. Biomol. Struct.* **1992**, *21*, 349.

(11) Song, S.; Asher, S. A.; Krimm, S.; Shaw, K. D. *J. Am. Chem. Soc.* **1991**, *113*, 1155.

(12) (a) Regan, J. J.; Bilio, A. J. D.; Langen, R.; Skov, L. K.; Winkler, J. R.; Gray, H. B.; Onuchi, J. N. *Chem. Biol.* **1995**, *2*, 489. (b) Langen, R.; Chang, I. Jy.; Germanas, J. R.; Gray, H. B. *Science* **1995**, *268*, 1733.

(13) Northrup, S. H. In *Protein Electron Transfer*; Bendall, D. S., Ed.; Bios Scientific: Oxford, 1996; pp 69−98.

(14) (a) Zhou, J. S.; Granada, E. S. V.; Leontis, N. B.; Rodgers, M. A. J. *J. Am. Chem. Soc.* **1990**, *112*, 5074. (b) Zhou, J. S.; Rodgers, M. A. J. *J. Am. Chem. Soc.* **1991**, *113*, 7728.

S0002-7863(97)02492-X CCC: $14.00

undergoing electrostatic interactions with the eight carboxylate residues disposed around the periphery of the uroporphyrin. Molecular modeling showed that a low-energy configuration placed the uroporphyrin over the lysine patch such that the two porphyrin π-planes were approximately orthogonal to each other and that the heme edge to uroporphyrin center distance was 7.8 Å. Alterations in driving force were achieved by changing the metallo substituent in the two tetrapyrroles. The intracomplex rate constants for the photoinduced forward electron transfer and the thermal back-transfer were measured as a function of driving force. The latter showed clear evidence for a Marcus inverted region with $\lambda = 0.7$ eV, whereas the former showed only a Marcus normal region after which the ln k_{ET} vs $-\Delta G^0$ plot showed a plateau at >0.8 eV driving force. To explain this driving force independent region, a two-step gating mechanism was invoked in which a surface-diffusion step was deemed to precede the electron transfer step. At the higher end of the driving force scale, this putative diffusion requirement became rate-determining.

In the present study there has been an attempt to use the same Coulomb-based electrostatic self-assembly principles to construct a model unit bearing resemblance to the cofactor and its immediate protein environment to allow an assessment of the role played by local diffusion. In this case, pentapeptides consisting of a string of four glutamic acid (Glu) residues terminated either by tryptophan (Trp) or tyrosine (Tyr) moieties were constructed using solid-phase peptide synthesis. The deprotonated carboxylic acid residues of the four Glus were postulated to act as an ion-pairing site for a tetracationic Pd(II) porphyrin, thus bringing the target (Tyr or Trp) moiety in proximity to the porphyrin and setting up the possibility of an intracomplex electron transfer event subsequent to photoexcitation of the porphyrin into an appropriate excited state. An additional factor of interest would be that the Tyr and Trp residues have a pH-dependent reduction potential, thereby allowing a pH-induced alteration of the driving force for the electron transfer event.

Experimental Section

Materials. Fmoc-protected L-amino acid derivatives (Fmoc-L-Tyr-(tBu)-OH, Fmoc-L-Trp(tBoc)-OH, and Fmoc-L-Glu(OtBu)-OH), activation reagents (DIPICDI and HOBt), and Fmoc-L-Glu(OtBu)-PEG−PS were Millipore peptide synthesis reagents. Ether (HPLC grade), cleavage reagent TFA, and methyl-d_3 alcohol (*d* 99.9% atom) were purchased from Sigma-Aldrich. DMF 99%, L-tyrosine 99%, and L-tryptophan 99% were obtained from Lancaster; DCM (certified ACS) from Fisher Scientific; and piperidine 99% from Aldrich. Palladium-(II) tetrakis(*N*-methyl-4-pyridyl)porphyrin, Cl salt $(Pd(II)TMPyP)^{4+}$ and its Zn analog were purchased from Mid-Century Chemicals.

Methods. Potassium dihydrogen phosphate and sodium hydrogen phosphate in equal proportions were used to make up the aqueous buffer solutions (10 mM). Porphyrin concentrations were determined from their absorbance at the Soret maxima, recorded in dilute neutral aqueous solutions. Molar extinction coefficients, ϵ (417 nm) = 158×10^3 M^{-1} cm^{-1} for $Pd(II)TMPyP^{4+}$ and ϵ (560 nm) = 16×10^3 M^{-1} cm^{-1} for $Zn(II)TMPyP^{4+}$ were used.[15,16] The pH was measured with a calibrated Corning ion analyzer (Model 250). Proton NMR spectra were recorded on a Varian Gemini 200 MHz spectrometer using deuterated solvent. Absorption spectra were recorded on a GBC 918 UV−vis rapid scan spectrophotometer. Fluorescence spectra were obtained with a Perkin-Elmer LS-5B luminescence spectrometer. HPLC measurements were carried out with a Waters Model 994 under the following conditions: C18 YCM-Pack column (QDS-AQ 150 × 4.6 mm i.d., S-5 m, 120 Å), the mobile phase was 10% (0.1% TFA in methanol) and 90% (0.1% TFA in water). Molecular weights were determined by electrospray mass spectrometry (University of Michigan, Ann Arbor). The peptide synthesis was carried out with a Millipore 9050 *Plus* PepSynthesizer.

Synthesis of Glu4Tyr and Glu4Trp. The linear pentapeptides having the following sequences Glu-Glu-Glu-Glu-Tyr and Glu-Glu-Glu-Glu-Trp were assembled via standard solid-phase peptide synthesis.[17] This stepwise construction of attaching a peptide to an insoluble polymer support involves the following steps: deblocking, washing, activation−coupling, and finally cleavage and deprotection.

In our synthesis Fmoc-protected L-amino acid derivatives; namely, Fmoc-L-Glu(OtBu)-OH, Fmoc-L-Tyr(tBu)-OH, and Fmoc-L-Trp(tBoc)-OH were used. During the synthesis, the N-termini of these amino acids are "temporarily" protected with the Fmoc group while the reactive side chains are "permanently" protected. The tyrosine hydroxyl reactive group was protected as its *tert*-butyl ether, the tryptophan reactive group was protected as a *tert*-butyloxycarbonyl and the glutamic carboxylate group was protected as its *tert*-butyl ester. This protection is essential to inhibit side chain reactions. The solid support used was Fmoc-L-Glu(OtBu)-PEG−PS, a poly(ethylene glycol)-*graft*-polystyrene copolymer with a Fmoc and active side-chain-protected glutamic acid attached to it via a PAC (peptide acid) linker.

Deblocking (removal) of the Fmoc groups (α-amino protecting groups) was achieved with 20% piperidine in DMF. Activation of the incoming amino acid was made with a mixture of DIPICDI (0.6 M/DMF) and HOBt (0.6M/DMF) using the *dual syringe* dissolution method (single activation). The activated amino acid was subsequently coupled to the support-bonded amino acid. During each step, excess reagents were removed through washing with DMF (following deblocking step) and DCM (following the coupling step).

Upon completion of the synthesis, the support-bound peptide was removed from the synthesizer and thoroughly dried overnight. Cleavage and deprotection were achieved by exposure to a TFA−H_2O (95%−5% v/v) cocktail for 2 h. The TFA−H_2O mixture removed the side chain protecting groups and also cleaved the bond anchoring the peptide to the support. The cleavage mixture (peptide−TFA−H_2O−support−protecting groups−byproducts) was filtered through a small piece of glass wool introduced into the neck of a 9 in. Pasteur pipette to retain the support particles. The recovered filtrate (peptide solution) was then added dropwise to a 10-fold excess of cold diethyl ether solution in acetone−dry ice bath. A white precipitate appeared in the ether solution as the drops hit the surface. Once the peptide had completely precipitated, it was collected by filtration, washed three times with diethyl ether, and dried under vacuum.

The peptides were characterized by UV absorption, fluorescence, HPLC, ^{1}H NMR, and electrospray mass spectrometry.

Transient Absorption Measurements. Flash photolysis experiments were performed with the second harmonic (532 nm) of a Continuum Surelite I Q-switched Nd:YAG laser which provided 6 ns pulses. Transient absorbances were monitored at right angles to the laser beam using a computer-controlled kinetic spectrometer which has been described elsewhere.[18] Solutions were argon saturated prior to each measurement.

Electrochemistry. Cyclic voltammetry (Electrochemical Analyzer, BAS-100A) was used to measure the reduction potential of tyrosine, tryptophan, and the oligopeptides at different pH values. For each measurement, the compound (0.5 mM) was dissolved in water containing KCl (0.2 M) and buffer (5 mM KH_2PO_4/5 mM Na_2HPO_4) and purged thoroughly with argon. A glassy carbon working electrode, highly polished prior to each measurement, was used in conjunction with Ag/AgCl reference electrode and a Pt counter electrode.

Abbreviations: Glu, glutamic acid; Tyr, tyrosine; Trp, tryptophan; Fmoc, fluorenylmethoxycarbonyl; *t*-Bu, *tert*-butyl; OtBu, *tert*-butoxy ester; DIPICDI, *N*,*N*-diisopropylcarbodiimide; HOBt, 1-hydroxybenzotriazole; PEG−PS, poly(ethylene glycol)−polystyrene; DMF, *N*,*N*-dimethylformamide; TFA, trifluoroacetic acid; DCM, dichloromethane.

Results

Peptide Characterization. Analytical HPLC showed the products Glu4Tyr and Glu4Trp as single peaks. Electrospray

(15) Brun, A. M.; Harriman, A. *J. Am. Chem. Soc.* **1994**, *116*, 10383.
(16) Kalyanasundaram, K. *Inorg. Chem.* **1984**, *23*, 2453.
(17) Merrifield, B. In *Peptides: Synthesis, Structure, and Applications*; Gutte, B., Ed.; Academic: New York, 1995.
(18) Rihter, B. D.; Kenney, M. E.; Ford, W. E.; Rodgers, M. A. J. *J. Am. Chem. Soc.* **1993**, *115*, 8146.

Table 1. ^{1}H Chemical Shift (δ ppm) and Coupling Constant (J, Hz) for Glu4Tyr in CD_3OD

residue	αH	βH	γH	aromatic
Glu	4.42 (m) 4.29[a]	1.96 (m) 1.97[a]	2.42 (m) 2.31[a]	
Tyr		3.28 (m)[b]		2,6 H, 7.10 (J = 8.4 Hz) 7.30[a] 3,5 H, 6.77 (J = 8.4 Hz) 6.86[a]

[a] Data from ref 24. [b] Overlap with solvent peak.

mass spectrometry showed the molecular weight of the parent ion in the Tyr analog as 697.3 g mol^{-1} (compared to a calculated one of 697.6 g mol^{-1}) and 720.5 g mol^{-1} for the Trp variant (compared to a calculated value of 720.68). Proton NMR data for the two oligopeptide products are shown in Tables 1 and 2.

The UV−visible absorption spectra of both free tyrosine and Glu4Tyr in buffered aqueous solutions (pH = 7) are shown in Figure 1. A close correspondence is observed between the two spectra, including similar maxima near 222 and 275 nm (± 0.2 nm) and fine structure details within the wavelength range 260−290 nm (inset, Figure 1).

The fluorescence spectra of free tyrosine (20 μM) and Glu4Tyr (20 μM) are displayed in Figure 2. Spectra were taken at matched absorbances of 0.08 at an excitation wavelength of 230 nm for both compounds to ensure the same number of photons absorbed. Both spectra consist of a single, unstructured band at 307 nm (±2.5 nm). However, the relative quantum yield of fluorescence when tyrosine was incorporated within the peptide linkage was clearly very much less (25%) than for the free monomer.

Redox potentials for one-electron oxidation of free tyrosine and tryptophan have been determined by cyclic voltammetry at different pH.[19] In the range pH = 2 to pH = 10, the redox potential E^0 was shown to decrease linearly with increasing pH.[19] To establish whether the coupling of tyrosine and tryptophan to a string of glu residues affects their reduction potential, this property was measured for the two oligopeptides as a function of pH. A typical voltammogram is displayed in Figure 3 (inset) for pH = 7.0. No peaks were observed in the reverse scan, probably because the oxidation product is unstable with respect to radical dimerization of tyrosyl and tryptophan residue radicals.[20] Under such conditions,[21] the observed peak potential (E_p) is related to the redox potential E^0 by

$$E_p = E^0 - 0.9(RT/nF) + (RT/3nF)\ln(2kCRT/3nvF)$$

where C is the concentration, v the potential scan rate, and k is the rate constant for the bimolecular chemical reaction. E^0 was determined for the free amino acids and the oligopeptides at different pH values. The results are displayed in Figure 3, where it can be seen that the redox properties of the target amino acids are not affected by the peptide environment, suggesting that the terminal tyrosyl residue environment within the peptide is probably similar to that of the monomers in solution.[22]

Porphyrin−Peptide Mixtures. (A) Ground State Spectra. UV−vis spectra of aqueous (pH = 7) solutions of Pd(II)-TMPyP^{4+} (12 μM) in the absence and presence of Glu4Tyr are shown in Figure 4. As the peptide concentration increased, the Soret band underwent a red shift with a concomitant decrease of the absorbance at maximum. However, at high peptide concentrations (above 500 μM), the absorption at λ_{max} increased again. The inset in Figure 4 shows similar behavior for the Q-bands. Similar spectral behavior was noted for the Trp variant.

(B) Pd(II)TMPyP^{4+} triplet state kinetics. Argon-saturated aqueous solutions of Pd(II)TMPyP^{4+} (10 μM) at pH = 7, irradiated with 6 ns pulse at 532 nm light, showed in-pulse formation of a transient absorption with λ_{max} = 460 nm, the decay of which was strictly monoexponential with a decay rate constant of 7×10^3 s^{-1}. In accordance with the literature and expectations, this transient, which decays more rapidly in the presence of oxygen, was assigned to the triplet (T_1) state of porphyrin. When one of the pentapeptides was present in the solution, the kinetic profile was changed significantly, the decay becoming faster and markedly nonexponential and the initial intensity was reduced from that in the absence of peptide (vide infra). The decay was best described by the sum of two exponential terms as shown by the typical time profile displayed in Figure 5. For the fast decay component, the evaluated rate constant was found to be independent of the peptide concentration (Figure 6). The mean concentration-independent value was $(6.6 \pm 0.2) \times 10^6$ s^{-1} for the Tyr variant and $(1.4 \pm 0.15) \times 10^7$ s^{-1} for the Trp analog. The slow contributor to the decay profile (k_s) showed a linear increase in value within the peptide concentration range investigated (0−120 μM) and a bimolecular rate constant of $(6.2 \pm 0.3) \times 10^9$ M^{-1} s^{-1} was evaluated that was independent of which target amino acid was attached to the Glu string (Figure 6).

(C) Effect of pH on the Porphyrin Triplet Kinetics. Laser pulse excitation of solutions of Pd(II)TMPyP^{4+} (8 μM) in the presence of Glu4Tyr (94, 60, and 30 μM) and Glu4Trp (93 μM) was carried out at a series of pH values in the range 2.8−10.[23] The rate constants of both fast and slow components of the triplet porphyrin decay changed with pH. Figure 7 shows the pH dependence of the fast component. These data are replotted in Figure 8, where the abscissa is now ΔE^0, computed from the potential data shown in Figure 3 with the assumption that the potential for the porphyrin reduction is independent of pH.

(D) Effect of Peptide Concentration on the Photophysics of Zn(II)TMPyP^{4+}. The experiments described above employing Pd porphyrin were repeated with the zinc-centered variant. The effect of Glu4Tyr concentration on the Zn(II)TMPyP^{4+} ground state absorption spectra was similar to that observed for Pd(II)TMPyP^{4+}; namely, a small red shift in the Soret band and a decrease of the porphyrin ground state extinction coefficient upon increasing the Glu4Tyr concentration. Similarly, the effect of peptide concentration on Zn(II)TMPyP^{4+} triplet state decay was investigated at pH = 7. In the absence of Glu4Tyr, the triplet decays according to a single exponential ($k = 1.6 \times 10^3$ s^{-1}). In the presence of Glu4Tyr, single-exponential kinetics were also observed, even at oligopeptide concentration up to 1.04 mM. Repeating these experiments at pH = 10.8 now showed that the triplet decay became double exponential (Figure 9). The slower decaying component was again dependent on the concentration of the oligopeptide (bimolecular rate constant evaluated as 3.6×10^9 M^{-1} s^{-1}),

(19) Harriman, A. *J. Phys. Chem.* **1987**, *91*, 6102.
(20) Hawley, D.; Adams, R. N. *J. Electroanal. Chem.* **1994**, *8*, 163.
(21) Nicholson, R. S. *Anal. Chem.* **1965**, *37*, 667.
(22) Values of $k = 6.0 \times 10^8$ M^{-1} s^{-1} for the combination of monomeric Tyr radicals and $k = 3.2 \times 10^8$ M^{-1} s^{-1} for the combination of monomeric Trp radicals[19] were employed herein to calculate E^0 values for the pentapeptides. Even in the unlikely event that the actual values for these radical reactions are lower by 1 order of magnitude, the relative error on the computed E^0 values would be near 1.5% (ca. 14 meV), which is within the error of the E_p measurement.

(23) Absorptiometric measurements showed that holding the metalloporphyrin solutions at pH = 2.8 for several hours (sufficient for the kinetic determinations) resulted in no loss of metal center.

Table 2. Chemical Shift (δ ppm) and Coupling Constant (J, Hz) for Glu4Trp in H_2O-D_2O (70/30, v/v)

residue	NH	αH	βH	γH	aromatic
Glu	8.43 (d, $J = 7.2$ Hz)	4.26 (m)	1.97 (m)	2.31 (t, J = 6.8 Hz)	
	8.33 (d, $J = 7.2$ Hz)		1.84 (m)	2.40 (m)	
Trp	8.37[a]	4.29[a]	1.97[a]	2.31[a]	
	8.25 (m)	4.75[b]	3.36 (d, $J = 6.8$ Hz)		NH: 10.17 (s), 10.22[a]
	8.09[a]				4H: 7.53 (d, $J = 9.6$ Hz), 7.65[a]
					7H: 7.48 (d, $J = 9.6$ Hz), 7.50[a]
					2H: 7.28 (s), 7.24[a]
					6H: 7.23 (t, $J = 9.2$ Hz), 7.24[a]
					5H: 7.11 (t, $J = 9.2$ Hz), 7.17[a]

[a] Data from ref 24. [b] Overlap with solvent peak.

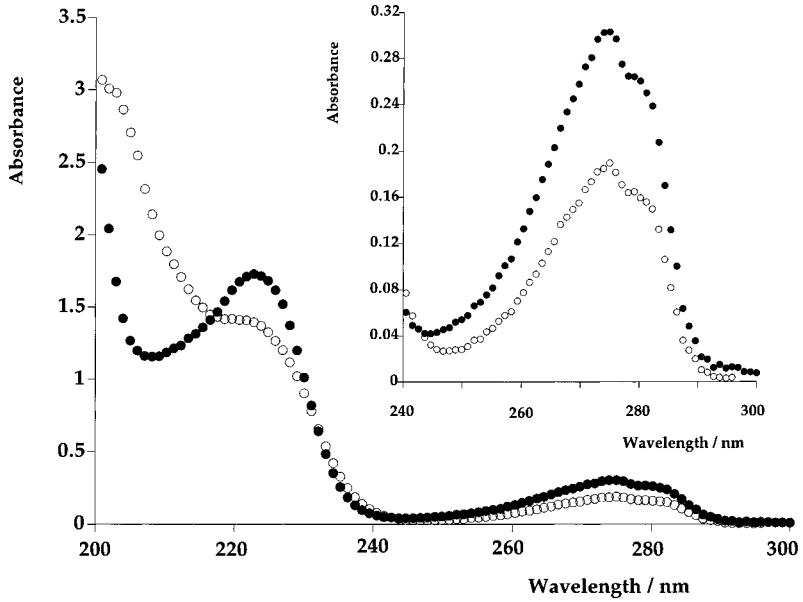

Figure 1. Ground state absorption spectra of tyrosine (●) and Glu4Tyr (○) in neutral buffered aqueous solutions, [tyrosine] = 20 μM and [Glu4Tyr] = 20 μM. Inset: absorption spectra in the range 240−300 nm.

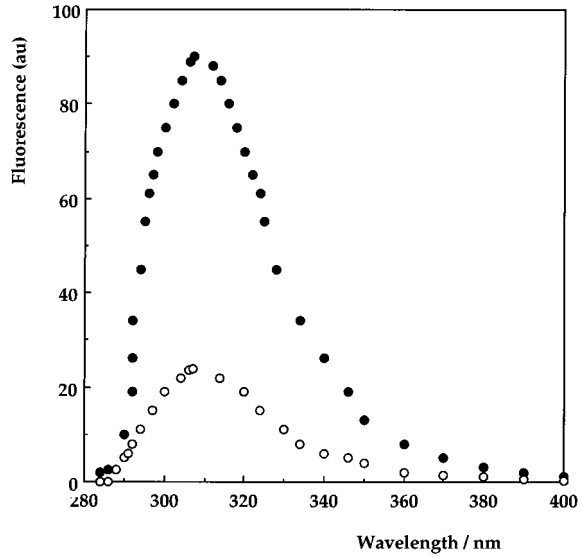

Figure 2. Fluorescence spectra of tyrosine (●) and Glu4Tyr (○) in neutral buffered aqueous solutions. Both tyrosine and Glu4Tyr absorbance were matched (OD = 0.08 at λ_{exc} = 230 nm).

whereas the fast component of the decay was concentration independent with a first-order rate constant of $(5 \pm 0.4) \times 10^6$ s^{-1} (Figure 10).

Fluorescence emission from aqueous solutions (pH = 7) of Zn porphyrin (5.6 μM) was measured at different Glu4Tyr concentrations. The excitation wavelength used was 563 nm (±2.5 nm), and measurements were performed under constant photon absorption conditions. A plot of the relative fluorescence quantum yield (I/I_0), viz., the fluorescence intensity in the presence vs the absence of Glu4Tyr is shown in Figure 11, where it can be seen that the singlet state Zn(II)TMPyP^{4+} fluorescence is not quenched by the Glu4Tyr ground state.

Discussion

Oligopeptide Characteristics. The observed chemical shift for Tyr, Trp, and Glu protons in oligopeptides (Tables 1 and 2) are in excellent agreement with those reported in the literature.[24] Also, the single peaks displayed in HPLC measurement along with the close correspondence between the calculated molecular weights and those determined by electrospray mass spectrometry indicate that the synthesized pentapeptides are of >97% purity.

The UV−vis absorption spectrum of tyrosine has been shown to have two major bands in the wavelength region between 200 and 300 nm.[25,26] The lowest energy singlet electronic transition is due to the ^1L_b band having a maximum near 277 nm and the much stronger ^1L_a band near 223 nm. As the spectra in Figure 1 show, both free Tyr and the tyrosyl residue in Glu4Tyr in buffered aqueous solutions display close similarity. In aqueous solutions, aromatic alcohols are well-known to be associated with solvent molecules; if stronger acceptors than water are present, these will compete with water molecules in hydrogen-bonding interactions, thereby causing red shifts in the absorption spectra.[27,28] At pH = 7, the carboxylate groups in side chains

(24) Bundi, A.; Wuthrich, K. *Biopolymers* **1979**, *18*, 285.
(25) Beaven, G. H.; Holiday, E. R. *Adv. Protein Chem.* **1952**, *7*, 319.
(26) Wetlaufer, D. B. *Adv. Protein Chem.* **1962**, *17*, 303.
(27) Chignell, D. A.; Gratzer, W. B. *J. Phys. Chem.* **1968**, *72*, 2934.

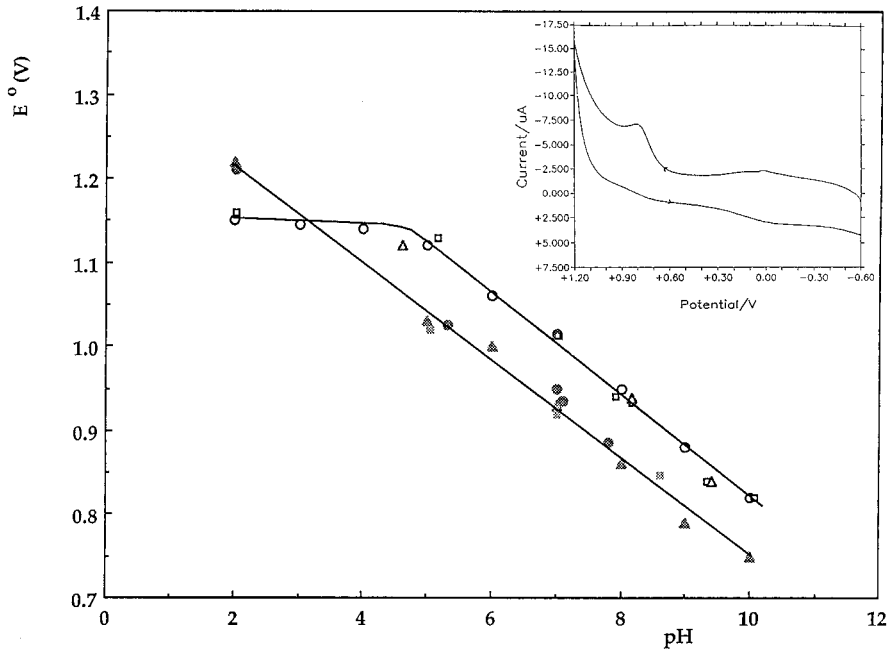

Figure 3. Plot of measured E^0 vs pH for tryptophan ○ (ref 19) and □ (our data); for tyrosine ▲ (ref 19) and ■ (our data); for Glu4Trp (△); and for Glu4Tyr (●). Inset: Typical cyclic voltammogram recorded for Glu4Tyr (0.5 mM) in neutral water. Plots of peak potential vs log v were linear.

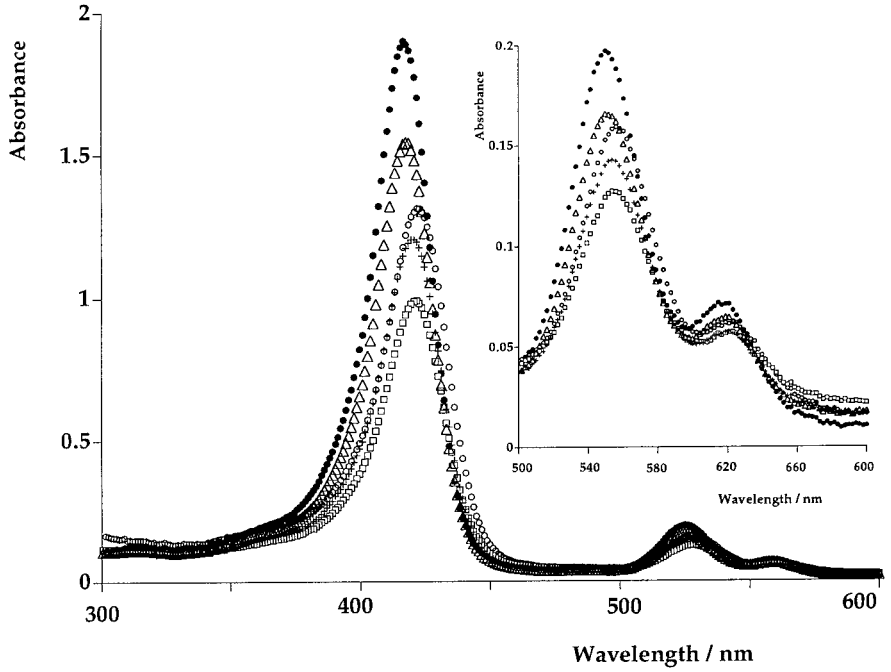

Figure 4. Ground state absorption spectra of Pd(II)TMPyP^{4+} (12 μM) in buffered aqueous solutions (pH = 7): ● (0 μM, λ_{max} = 416.3 nm); △ (21 μM, λ_{max} = 417.4 nm); + (262 μM, λ_{max} = 420.5 nm); □ (623 μM, λ_{max} = 421.6 nm); and ○ (1928 μM, λ_{max} = 421.6 nm). Inset: ground state absorption in the range 500−600 nm.

of the glutamic acid residues are deprotonated and could compete with water molecules in forming hydrogen bonds with the tyrosyl hydroxyl group. However, the absence of any shift in the Glu4Tyr ground state absorption spectra seems to refute such a suggestion. At pH = 7 there is no evidence for the deprotonation of the tyrosyl hydroxyl group incorporated in the pentapeptide matrix; otherwise, the 227 nm absorption peak would be shifted to 294 nm and the 223 nm peak to 240 nm.[25] Deprotonation of this residue is known to affect the lower energy absorption band of Tyr in such a way that the vibrational structure is lost.[25,26] As shown in Figure 1, the fine structure details within the 260−290 nm region observed with free Tyr are preserved in Glu4Tyr. This may be an indication that carboxylate side chain groups are sterically (in terms of distance and/or relative orientation to the tyrosyl residue) inhibited from the optimal hydrogen-bonding configurations with the Tyr hydroxyl group in Glu4Tyr.

The fluorescence spectrum of tyrosine, both in aqueous solutions and when bound into proteins and polypeptides, usually consists of a single, unstructured band with a maximum between 303 and 305 nm.[29] Thus, the Tyr fluorescence appears to be relatively insensitive to the local environment. However, the quantum yield of the fluorescence of the tyrosyl residue is extremely sensitive to the nature and structure of its molecular

(28) Willis, K. J.; Szabo, A. G. *J. Phys. Chem.* **1991**, *95*, 1585.

(29) *Topics in Fluorescence Spectroscopy, Volume 3, Biochemica*; Lakowicz, J. R., Ed.; Plenum: New York, 1992.

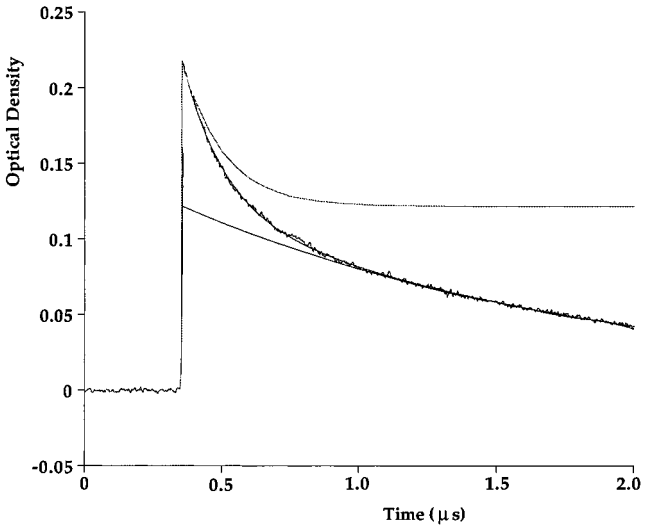

Figure 5. Decay profile of the absorbance change at 460 nm following pulsed 532 nm excitation of an argon-saturated neutral aqueous solution of Pd(II)TMPyP^{4+} (10 μM) in the presence of Glu4Tyr (94 μM).

environment.[30] These common features are well illustrated in Figure 2, where it is seen that the relative quantum yield of fluorescence undergoes a significant lowering when the tyrosine is incorporated into the pentapeptide. The quenching of the fluorescence of tyrosyl residues in peptides has been the subject of much discussion. A number of different mechanisms have been proposed which focus on the role of the local environment of the tyrosyl residue in a protein or peptide. These are grouped into different types as defined by interactions with a specific moiety or quenching by a specific mechanism and may involve (i) the peptide bond, specifically the carbonyl group;[31−35] (ii) resonance energy transfer;[36,37] and (iii) amino acid chains which may act as proton donors or acceptors or as partners in hydrogen bonding.[32,38−43] The quenching shown in Figure 2 may be caused by one or more of these mechanisms. However, a mechanism involving hydrogen bonding between the tyrosyl residue and an amino acid chain may be discarded since no evidence for such bonding was observed in the Glu4Tyr absorption spectra (Figure 1). Cowgill[41] classified tyrosyl residues in proteins according to their relative quantum yield, R_{Tyr}, and the probable effects of the environmental conditions. For instance, he described type I quenching mechanism as due to tyrosyl residues exposed to hydrated peptide carbonyl groups for which $R_{Tyr} = 0.25-0.33$ (by comparison to free tyrosine in neutral aqueous solution taken as reference and for which $R_{Tyr} = 1$). Thus, according to this classification, the value of $R_{Tyr} = 0.25$ for Glu4Tyr may indicate that tyrosyl residues in the pentapeptide, when excited into the S_1 state, are sufficiently close to the carbonyl residues to undergo fluorescence quenching.

Transient Kinetics Studies. The primary hypothesis behind this research effort was that under appropriate solution conditions tetracationic porphyrins, such as those employed herein, would undergo ion pairing with the synthetic polyanionic oligopeptides Glu4Tyr and Glu4Trp, which are composed of a string of four glutamic acid residues with a target residue at the N-terminus and a free carboxylate group at the C-terminus. At pH = 7 the carboxylate residues will be deprotonated and thereby provide anionic sites to which the porphyrin can "associate" through Coulombic interactions. Thus, electrostatic interactions between the tetracationic and the anionic entities could lead to self-assembly of a complex having no driving force for assembly other than that provided by ion pairing. Taking the hypothesis one stage farther, it is possible to ponder the structural features of the ion pair. For example, the X-ray data for the porphyrin[44] show the four pyridinium nitrogen atoms at a distance of some 7.8 Å from the molecular center. This relatively fixed geometrical arrangement of the cationic centers provides a template onto which the carboxylates of the four Glu moieties may associate. It is supposed that there is enough conformational freedom in the peptide and its side chains to accommodate an arrangement in which one carboxylate residue is positioned in an ion-pairing configuration with one of the porphyrin cationic locations. Such a model would then place the oxidizable part of the target residue in proximity to the T_1 state of the porphyrin on account of the tether provided by the peptide link between the target (Trp or Tyr) and its Glu neighbor. The term proximity in this context is not meant to imply close contact; rather, the target and the porphyrin are confined within the same volume fragment of the solution (vide infra) and any putative chemical interaction between them will be akin to that between geminate pairs, viz., any diffusion requirement will be limited to a reorganization within a restricted space. For such a system, any interspecies reaction will show first-order kinetic behavior having no dependence on concentration of reactants. A schematic of a stylized ion pair is shown in Figure 12.

Evidence for ion association is provided by the effect on the ground state absorption of Pd(II)TMPyP^{4+} of increasing the pentapeptide concentration (Figure 4). The addition of peptide causes the Soret band to undergo a red shift, with a lessening of the absorption intensity at the band maximum. Without delving into the nature of the interaction that results in these effects, the effects themselves indicate that complexation between the components of the system is occurring in accordance with this hypothesis. Thus, ground state absorption spectral evidence clearly supports the existence of an ion-pair equilibrium, and the value of the equilibrium constant will determine the ratio of "free" to "complexed" porphyrin at any given oligopeptide concentration. Moreover, when the conditions are such that the equilibrium contains significant mole fractions of both free and complexed porphyrin, photoexcitation of the tetrapyrrolic π-system will produce two populations of porphyrin S_1 and then T_1 states: one that is localized within the complex and thus proximate to a tyrosine (or tryptophan) moiety of the oligopeptide and one that has no such preset organization. This situation is clearly reflected in the observation presented in Figure 5 and the compiled data shown in Figure 6. The fact that inclusion of target-containing oligopeptide into the solution converts what is initially a single-exponential T_1 decay with a lifetime of 125 μs without peptide into a biexponential decay which removes all T_1 from the system within 10 μs indicates that the peptide is seriously perturbing the Pd porphyrin excited state. That the fast triplet decay

(30) *Biochemical Fluorescence: Concepts;* Chen, R. F., Edelhoch, H., Eds.; Marcel Dekker: New York, 1976; Vol. 2.
(31) Cowgill, R. W. *Biochim. Biophys. Acta* **1967**, *133*, 6.
(32) Feitelson, J. *J. Phys. Chem.* **1964**, *68*, 391.
(33) Feitelson, J. *Photochem. Photobiol.* **1969**, *9*, 401.
(34) Cowgill, R. W. *Biochim. Biophys. Acta* **1970**, *200*, 18.
(35) Cowgill, R. W. *Biochim. Biophys. Acta* **1968**, *168*, 431.
(36) Weber, G. *Biochem. J.* **1960**, *75*, 345
(37) Cowgill, R. W. *Biochim. Biophys. Acta* **1966**, *112*, 550.
(38) Teale, F. W. J. *Biochem. J.* **1960**, *76*, 381.
(39) Cowgill, R. W. *Biochim. Biophys. Acta* **1965**, *109*, 536.
(40) Weber, G.; Rosenheck, K. *Biopolymers* **1964**, *1*, 333.
(41) Cowgill, R. W. *Biochim. Biophys. Acta* **1968**, *168*, 417.
(42) Longworth, J. W. In *Excited States of Proteins and Nucleic Acids*; Steiner, R. F., Weinryb, I., Eds.; Plenum: New York, 1971; pp 319−484.
(43) Cowgill, R. W. In *Biochemical Fluorescence: Concepts 2*; Chen, R. F., Edelhoch, H., Eds.; Marcel Dekker: New York, 1976; pp 441−486.
(44) Ford, K.; Fox, K. R.; Neidle, S.; Waring, M. J. *Nucleic Acids Res.* **1987**, *15*, 2221.

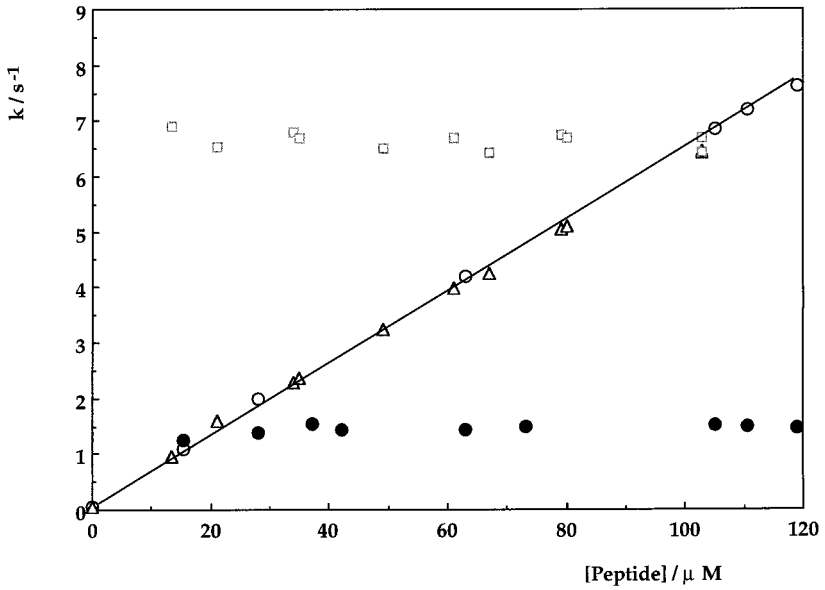

Figure 6. Variation of the fast component k_f and the slow component k_s of Pd(II)TMPyP^{4+} (10 μM) triplet decay in argon-saturated buffered aqueous solutions (pH = 7) in the presence of Glu4Tyr □ (10^{-6} k_f), △ (10^{-5} k_s); and Glu4Trp ● ($10^{-7}k_f$) and ○ ($10^{-5}k_s$).

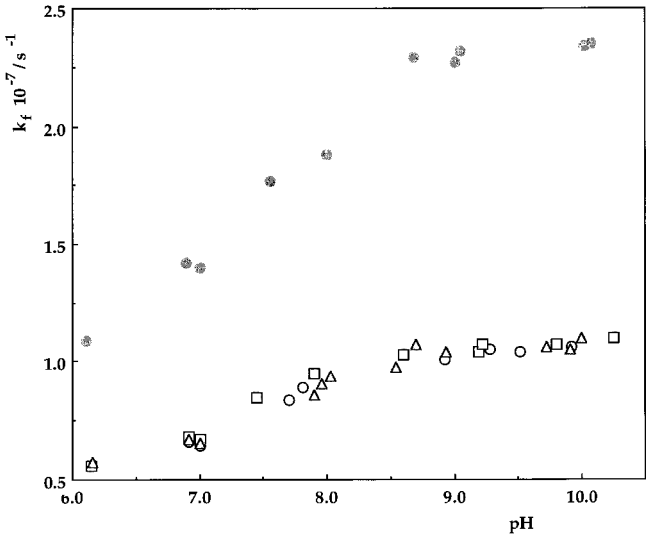

Figure 7. pH dependence of the fast component (k_f) decay rate constant for Pd(II)TMPyP^{4+} (10 μM) at different Glu4Tyr concentrations △ (94 μM), ○ (60 μM) and □ (30 μM); and Glu4Trp ● (93 μM).

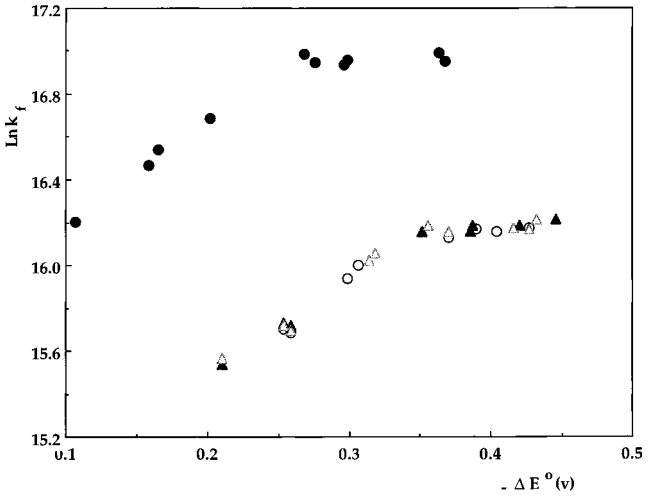

Figure 8. Driving force dependence of the fast component (k_f) decay rate constant for PdTMPyP^{4+} (10 μM) at different Glu4Tyr concentrations △ (94 μM), ○ (60 μM) and ▲ (30 μM); and Glu4Trp ● (93 μM).

component has a peptide concentration-independent rate constant (6.6×10^6 s^{-1} for Tyr and 1.4×10^7 s^{-1} for Trp) whereas the slower one is concentration dependent and first order in peptide concentration (up to 120 μM) and therefore bimolecular, intimates that the hypothetical ion-pair equilibrium has validity. This is supported by the observations that the relative contributions of the "fast" and "slow" processes increase upon increasing oligopeptide concentration. To a first approximation this behavior can be represented by Scheme 1.

In Scheme 1, A represents the porphyrin, B the peptide, and the square brackets indicate the ion-pair complex; k_T and k_{TC} are intersystem crossing rate constants of the porphyrin in the two systems; k_B represents the bimolecular rate constant for the reaction between the T_1 state of the free porphyrin to produce the encounter complex [A(T_1):B]; k_Q is the rate parameter governing the as-yet-unspecified quenching process; and k_G is the rate parameter governing a reaction that regenerates the starting materials within the solvent cage, which can then establish equilibrium with the uncomplexed species. It is possible that the species formed by excitation of the ground state complex and the diffusion together of the separate T_1 and peptide entities may not be of identical configuration (vide infra). However, it is assumed that they are at least kinetically similar. In the channel that is initiated by photoexcitation of the complex, k_Q is the rate constant that was shown to be independent of peptide concentration. This follows because the intersystem crossing reaction in Pd(II) porphyrins is extremely rapid and has been reported as restricting S_1 lifetimes to ca. 20 ps.[45]

The slower contributor to the T_1 decay arises from that fraction of the equilibrium ground state population that is not involved in complex formation prior to the excitation pulse but which undergoes diffusive formation of an encounter complex with free peptide molecules. This process is governed by the bimolecular rate constant k_B, which was evaluated as 6.2×10^9 M^{-1} s^{-1} for both peptides, a value which is in the realm of diffusion-limited rate constants. Since the slower process is observed to be to the first order in peptide concentration within the range of concentration investigated (up to 120 μM), the quenching reaction within the encounter complex must have a rate parameter that is much greater than the product k_B[B], viz., the diffusion process determines the reaction rate. This is the

(45) Collis, J. B.; Gouterman, M.; Jones, Y. M.; Henderson, B. H. *J. Mol. Spectrosc.* **1971**, *29*, 410.

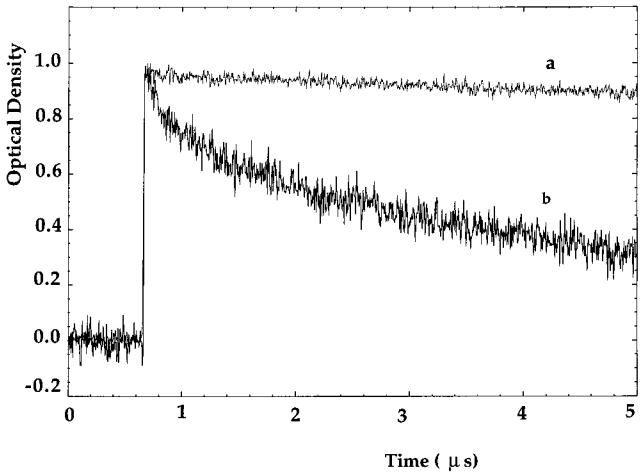

Figure 9. Normalized decays of the absorbance change at 480 nm following pulsed 532 nm excitation of an argon-saturated aqueous solution of Zn(II)TMPyP^{4+} (10 μM) in the presence of Glu4Tyr (52 μm) at pH = 7 (a) and pH = 10.8 (b).

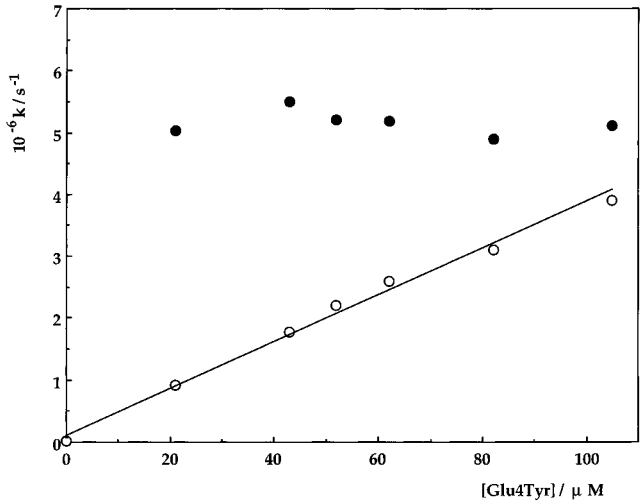

Figure 10. Variation of the fast component k_f (●) and the slow component $10k_s$ (○) of Zn(II)TMPyP^{4+} (5 μM) at pH = 10.8 with Glu4Tyr concentration.

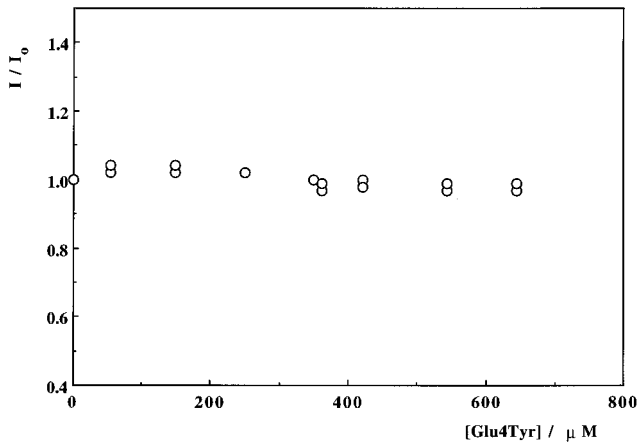

Figure 11. Plot of the relative fluorescence quantum yield (I/I_0) of Zn(II)TMPyP^{4+} (5.6 μM) at different Glu4Tyr concentrations. All measurements were made at matched OD = 0.08 (λ_{exc} = 563 ± 2.5 nm) in buffered solution, pH = 7.

minimum condition that suffices to explain the observations depicted in Figures 5 and 6. At this juncture, it is relevant to note that at pH = 3, when the oligopeptide was present at a concentration of 52 μM, the triplet state decayed with a rate

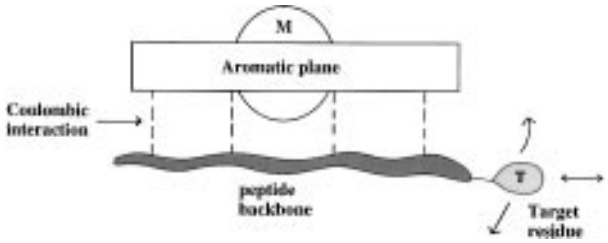

Figure 12. Schematic representation of an ion-pair pentapeptide−porphyrin complex.

Scheme 1

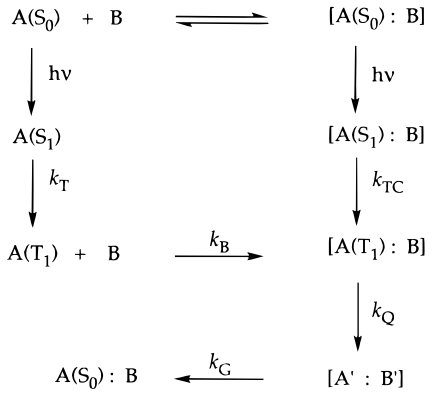

constant of 2.6×10^4 s^{-1}, a value that is ca. 3 times that found for the triplet decay constant in the absence of the peptide. This may be understood through the fact that the carboxylate side chains of the Glu residues are protonated at this low pH value, thereby removing the interaction responsible for ion pairing. That the triplet decay constant is somewhat higher than that in the absence of Glu4Tyr is probably a consequence of a weak bimolecular quenching between the triplet state and the fully protonated peptide.

Having shown that the ion-pair complexation hypothesis has credence, it is appropriate to turn to the question of the mechanism by which the triplet state of the porphyrin is being quenched by the oligopeptide. As indicated earlier, tyrosine and tryptophan are among the most easily oxidized amino acids. Harriman[19] has shown that the reduction potentials of tyrosine and tryptophan vary linearly with pH. The data reported herein (Figure 3) confirm the Harriman results for the target monomers and additionally demonstrate that binding to a string of four Glu residues has no effect on the reduction potentials of the oxidized Trp and Tyr species. At pH = 7 the reduction potential for the tyrosine radical cation is 0.93 V and that of the T_1 state of Pd(II)TMPyP^{4+} is quoted as 1.18 V.[46] Thus, the standard potential difference for an electron transfer process from a tyrosyl residue to the porphyrin triplet state is $\Delta E^0 = 0.25$ V, and the formation of the tyrosyl radical cation under such conditions is thermodynamically favored. The same computation for the Trp variant (reduction potential of 1.0 V) yields $\Delta E^0 = 0.18$ V, providing a similar conclusion. To examine this further, the porphyrin triplet state decay in the presence of GluTyr and Glu4Trp was measured at a series of pH values in the range 2.8−10, where the E^0 values of the targets decline linearly with pH (Figure 3). Then, assuming that the reduction potential for the porphyrin T_1 state is invariant with pH, the values of ΔE^0 for the electron transfer process

(46) *Photochemistry of Polypyridine and Porphyrin Complexes*; Kalyanasundaram, K., Ed.; Academic: London, 1992.

$$A(T_1) + B \rightarrow A^- + B^+$$

were calculated to vary from 0.01 V at pH = 3 to 0.44 V at pH = 10 for the Tyr variant (Figure 7). As indicated earlier, the decay profile at pH = 3 showed no evidence of an intracomplex component ($k = 2 \times 10^4$ s^{-1}) because the Glu residues are protonated at that pH. However, as the pH was adjusted to be above 6, the decay profile was again double exponential, having a fast component with a decay rate constant which increased as the pH increased (Figure 7). In this pH range the reduction potential of the tyrosyl entity diminishes as the pH increases, thereby causing the oxidation of Tyr by the porphyrin triplet state to become thermodynamically more favorable. Similar observations were made for the Trp variant, except that the intracomplex rate constants were higher than in the case of the Tyr variant (vide infra). These data allowed construction of the plot presented in Figure 8, which shows that the intracomplex rate constant, i.e., the concentration-independent component, undergoes an increase as the pH-governed ΔE^0 for target oxidation increased. This is consistent with the proposal that the quenching of the porphyrin T_1 state involves an electron transfer event.

Further evidence for an electron transfer mechanism was obtained when Zn(II)TMPyP^{4+} was employed in place of the Pd(II) variant as the putative electron acceptor (Glu4Tyr only). The ground state absorption spectral behavior of peptide−Zn(II)-porphyrin mixtures indicated ion-pairing interactions exactly as seen in the case of the Pd(II) variant. It would be expected then that such complexes might show similar photokinetic behavior to those of the Pd complex. However, the reduction potential of the T_1 state of Zn(II)TMPyP^{4+} is listed as 0.78 V in aqueous solution,[46] some 400 mV lower that of the Pd porphyrin. At pH = 7, therefore, the value of $\Delta E^0 = 0.78 - 0.93 = -0.15$ V; hence the electron transfer process from tyrosyl is energetically unfavorable. Indeed, at pH = 7 the triplet state profile showed single exponential kinetics even at Glu4Tyr concentrations up to 1.04 mM.

As indicated above, the reduction potential of the tyrosyl system can be manipulated by changing the pH of the solution; thus at pH = 10.8, the reduction potential of the tyrosyl cation is shifted to 0.67 V, thereby putting the driving force for the electron transfer process at $\Delta E^0 = 0.09$ V, i.e., in the energetically favorable region. At this pH it was indeed observed that the Zn porphyrin T_1 decay profile was again double exponential, confirming that the intracomplex quenching can occur when the driving force for electron transfer is favorable. As Figure 10 shows, for the Zn porphyrin at pH = 10.8, the rate constant for the slow component of the triplet decay depended on the peptide concentration, whence a bimolecular rate constant of 3.68×10^9 M^{-1} s^{-1} could be evaluated. The fast component was concentration independent (*cf.* Pd porphyrin) with a mean value of 5.15×10^6 s^{-1} (Figure 10), which was close to the value found for the Pd porphyrin (6.6×10^6 s^{-1}) under similar pH conditions, although the driving forces are significantly different, being $\Delta E^0 = 0.44$ V for Pd(II) and $\Delta E^0 = 0.09$ V for the Zn case. This point will be referred to later. Nevertheless, the indications are that the process responsible for quenching of the porphyrin T_1 state is electron transfer from the target moiety to the porphyrin under favorable driving force conditions.

The above discussion has focused on the probability that electron transfer is the predominant quenching mode for deactivation of the T_1 state of the porphyrins by the adjacent oxidizable amino acid at the N-terminus of the oligopeptide. However, some of the evidence is seemingly less than supportive. For example, scrutiny of Figure 8 shows that the rate constant for intracomplex transfer increases with increasing (pH-dependent) driving force, after which it becomes level. However, Figure 3 shows that the value of the reduction potential of the target residue continues its linear decrease above pH values where the rate constants become pH (and thus driving force) independent. Thus, if electron transfer from the target amino acid is indeed the reason for the deactivation of the porphyrin T_1 state, (as the lower pH data would indicate), then the rate constant would be expected to continue to increase with increase in driving force, or even decline (thereby showing a Marcus-inverted region). The observed leveling off is unexpected. Nevertheless, such behavior is reminiscent of that reported in this laboratory earlier[14] in which it was shown that rate data for electron transfer reactions between metallouroporphyrin T_1 states and cytochrome-*c* (FeIII) followed a plot similar to that seen in Figure 8 (see Introduction). The similarity between the results of the earlier experiments and these reported here is intriguing; both concern electron transfer between an excited state of a metalloporphyrin and a reaction partner when the two are constrained within a preformed ion-pair complex; both show rate constant trends in which a Marcus normal region is followed by a driving force-independent region.

Kinetic phenomena of this kind often indicate a change in mechanism, in this case from a process governed by an energy barrier to electron transfer, to one that has different characteristics. At lower values of driving force the rate constant of an electron transfer process is modified via an activation free energy according to the Marcus relationship[2a]

$$\Delta G^{\ddagger} = (\Delta G^0 + \lambda)/4\lambda$$

where ΔG^0 is the standard free energy governing the reaction and λ is a reorganization energy term. What is observed here is that the increase in driving force causes the rate constant to reach a value where electron transfer is no longer rate-determining, a driving force-independent mechanism dominates, and a limit to the driving force-dependent region is attained. In bimolecular reactions between freely diffusing reaction partners, it is well documented that molecular diffusion through the medium creates a limiting condition for reaction rate constants. However, in this work, and in that concerning cytochrome *c* and uroporphyrins, the reacting system was assembled specifically to remove the confusing effects of the free diffusion. Thus, within the time window of the forward and reverse electron transfer event (ca. 1 μs), it is considered that the ion-pair complexes are undissociated.

However, the nature of the components of the complex are that the T_1 state of the putative acceptor (Pd porphyrin) is held in association with the Glu residues of the pentapeptide, and the other reaction partner tyrosine (or tryptophan) is connected to the latter by a peptide link. This tether has intrinsic conformational flexibility which assuredly permits some degree of segmental diffusion (Figure 12) and, moreover, ensures that prior to photoexcitation the target and porphyrin moieties are separated by a restricted distribution of distances. After excitation of the porphyrin molecule, segmental motions will serve to bring the partners to a configuration at which the electron jump can occur. This requirement for reorganizational diffusion is a random event and apparently imposes a limiting lifetime of ca. 10^{-7} s on the reaction in situations where the driving force no longer is the limiting factor. The apparent "slowness" of the 10^{-7} s value indicates that the diffusional requirement is not simply a bond rotation but rather the adventitious result of many rotations. Diffusive motion of this kind has been advocated during the transient formation of

weakly bound protein−protein complexes as a common feature of biological electron transfer.[13] It is not unlikely that similar diffusional searching is necessary in the kind of complexes that have been constructed here, although no independent evidence exists for this putative motion.

Other observations that require understanding appear in Figure 8. What is especially intriguing about the data presented there is that everywhere on the plot the intracomplex rate constants for the Trp peptide are higher than those for the Tyr variant. Yet in the ΔE^0-dependent region, the driving force for the Trp peptide is always lower. One of two influences could cause such an effect. The first requires the assumption that, in the ground state of the ion pair, Trp residues are, on average, closer to the porphyrin than are Tyr residues, thereby leading to a less stringent requirement for tethered diffusion. Support for such an assumption could be derived from the concept that the terminal phenolic group of Tyr is more hydrophilic than the terminal indole of Trp and prefers a situation where its environment is more aqueous, while the indole prefers to be proximate to the porphyrin π-system. The second influence that could be brought into this argument is that the oxidation of Tyr has different reorganization energy (λ) requirements to that of Trp. Such differences could again be supported by hydrophobicity considerations. At this time it is only possible to speculate about such things, but experiments are under way to measure the relevant λ values.

If electron transfer from the target amino acid to the triplet state of the porphyrin is indeed involved in deactivation of the excited state, it would be anticipated that the transient absorption spectrum at times after which the triplet state had decayed should display evidence for the presence of porphyrin radical anion and an oxidized target species. In fact, no such evidence could be found, an observation that could indicate that the loss of the radical pair state and concomitant repopulation of the ground state of the system must be significantly more rapid than the reaction that forms the radical pair. At pH = 7 this latter process has a lifetime of ca. 150 ns; therefore, a radical pair lifetime of say 20 ns or less would suffice to make it impossible to observe absorption of the electron transfer products. Such a lifetime is not surprising if one considers that the 150 ns value represents the time necessary for the ion-pair complex to undergo the limited segmental diffusion necessary for the forward electron jump. The electron return process, however, has no such requirement since the participants are conformationally prepared once the forward process has taken place. There is a spin-imposed barrier, however, since the radical pair was prepared in a triplet state configuration. Nevertheless, intersystem crossing rate constants leading to state lifetimes in the 20 ns region are not uncommon.

A final point concerns the experiments that were carried out to measure the effect of the addition of peptide on the quantum yield of fluorescence from the Zn(II) porphyrin. As Figure 11 shows, the quantum yield for fluorescence was independent of whether the porphyrin was complexed or not. At pH = 7 the driving force for an electron transfer reaction between the S_1 state of the Zn porphyrin and Tyr will be ca. 500 mV more favorable than that estimated above for the T_1 state as −0.15 V. Hence the singlet reaction will be favorable by ca. 350 mV, which is 100 mV more favorable than that involving the T_1 state of the Pd porphyrin at pH = 7. Yet no quenching of fluorescence was observed. It thereby becomes apparent that at these moderate driving forces electron transfer is not rapid enough to compete with the radiative process in the porphyrin which has a lifetime in the region of 2 ns. Thus the putative requirement of tethered diffusion prior to electron transfer means that only the long-lived species such as triplet states can succeed in causing photoinduced oxidation of the proximate peptide entity.

Acknowledgment. Support for this work was provided by NIH Grant CA46281 and by the Center for Photochemical Sciences, Bowling Green State University.

JA972492U